Titan's Atmospheric Temperatures, Winds, and Composition

F. M. Flasar, *et al.*

Science **308**, 975 (2005);
DOI: 10.1126/science.1111150

Titan's Atmospheric Temperatures, Winds, and Composition

F. M. Flasar,[1]* R. K. Achterberg,[2] B. J. Conrath,[3] P. J. Gierasch,[3] V. G. Kunde,[4] C. A. Nixon,[4] G. L. Bjoraker,[1] D. E. Jennings,[1] P. N. Romani,[1] A. A. Simon-Miller,[1] B. Bézard,[5] A. Coustenis,[5] P. G. J. Irwin,[6] N. A. Teanby,[6] J. Brasunas,[1] J. C. Pearl,[1] M. E. Segura,[7] R. C. Carlson,[2] A. Mamoutkine,[2] P. J. Schinder,[3] A. Barucci,[5] R. Courtin,[5] T. Fouchet,[5] D. Gautier,[5] E. Lellouch,[5] A. Marten,[5] R. Prangé,[5] S. Vinatier,[5] D. F. Strobel,[8]† S. B. Calcutt,[6] P. L. Read,[6] F. W. Taylor,[6] N. Bowles,[6] R. E. Samuelson,[4] G. S. Orton,[9] L. J. Spilker,[9] T. C. Owen,[10] J. R. Spencer,[11] M. R. Showalter,[12] C. Ferrari,[13] M. M. Abbas,[14] F. Raulin,[15] S. Edgington,[9] P. Ade,[16] E. H. Wishnow[17]

Temperatures obtained from early Cassini infrared observations of Titan show a stratopause at an altitude of 310 kilometers (and 186 kelvin at 15°S). Stratospheric temperatures are coldest in the winter northern hemisphere, with zonal winds reaching 160 meters per second. The concentrations of several stratospheric organic compounds are enhanced at mid- and high northern latitudes, and the strong zonal winds may inhibit mixing between these latitudes and the rest of Titan. Above the south pole, temperatures in the stratosphere are 4 to 5 kelvin cooler than at the equator. The stratospheric mole fractions of methane and carbon monoxide are $(1.6 \pm 0.5) \times 10^{-2}$ and $(4.5 \pm 1.5) \times 10^{-5}$, respectively.

Unlike other moons in the solar system, Titan has a substantial atmosphere and offers an interesting comparison with Earth and the other planets. Its pressure at the surface is 1.5 times Earth's, but its temperature is much colder, 90 to 94 K (*1*–*3*). Like Earth, Titan's atmosphere is primarily N_2, but CH_4 (not O_2) is the next–most abundant constituent. Dissociation of CH_4 and N_2 by ultraviolet sunlight and energetic electron impact leads to a rich mixture of organic compounds (*4*–*6*). Titan's winter polar atmosphere may be analogous to the terrestrial Antarctic ozone hole but with different chemistry. Infrared observations from the Voyager spacecraft indicated cold stratospheric temperatures, strong circumpolar winds, and an enhanced concentration of several organic compounds in the north-polar region, which was coming out of winter in 1980 to 1981 (*7*–*9*). This enhanced concentration suggests that the winter polar atmosphere was isolated from that at low latitudes. Titan has a 16-day period and rotates slowly, like Venus. Both have atmospheres that rotate globally much faster than their surfaces. Unlike Venus, however, Titan has a large seasonal modulation in its stratospheric temperatures and winds (*2*, *7*).

Here we summarize results from early Cassini orbiter observations of Titan by the Composite Infrared Spectrometer (CIRS). The observations were made on 2 July 2004 (flyby T0), shortly after Cassini was inserted into orbit around Saturn, and on 13 December 2004 (flyby TB). CIRS consists of two Fourier-transform spectrometers, which together measure thermal emission from 10 to 1400 cm^{-1} (wavelengths 1 mm to 7 μm) at an apodized spectral resolution selected between 0.5 and 15.5 cm^{-1} (*10*, *11*). The far-infrared interferometer (10 to 600 cm^{-1}) has a 4-mrad field of view on the sky. The mid-infrared interferometer consists of two 1×10 arrays of 0.3-mrad pixels, which together span 600 to 1400 cm^{-1}.

Like Earth, Titan has a well-defined stratosphere. It has been well characterized at altitudes up to ~225 km by Voyager radio-occultation and infrared observations (*1*, *7*, *8*) and also by the Infrared Space Observatory (*12*). Titan stellar occultations have been used to probe the mesosphere at altitudes of 300 to 500 km (*13*, *14*). In this region, the retrieved temperature profiles show great variability, possibly because of the influence of vertically propagating waves. The accuracy of the retrieved temperatures decreases at altitudes below ~300 km because of the uncertain contribution of aerosol absorption to the signal. None of these observations defined the stratopause, which is the maximum in the temperature profile separating the mesosphere from the underlying stratosphere. The stratopause temperature and its location are determined by the vertical variation of aerosol heating, infrared cooling to space by C_2H_6, and, to a lesser extent, heating of CH_4 in its near-infrared bands (*15*). At these altitudes, CH_4 is well mixed, but the aerosols tend to decrease with altitude and C_2H_6 increases slowly with altitude (*6*). The spatial resolution of the mid-infrared detector arrays allowed CIRS to observe Titan's atmosphere on the limb, where the line of sight extends through the atmosphere to deep space. In this mode, the altitude coverage and vertical resolution was determined by the array pixels (*11*). Figure 1A shows that vertical profiles up to the 0.01-mbar level (410 km) are feasible. At 15°S, a well-defined stratopause is evident near 0.07 mbar (310 km) with a temperature of 186 K.

CIRS mapped stratospheric temperatures over much of Titan (Fig. 1, B and C) in the second half of 2004, with its mid-infrared arrays in the nadir-viewing mode. This corresponded to early southern summer (solstice was in October 2002). The warmest temperatures were near the equator. Temperatures were moderately colder at high southern latitudes (by 4 to 5 K near 1 mbar), but they were coldest at high latitudes in the north, where it was winter. The thermal wind equation relates the variation of zonally averaged temperatures with latitude to the variation of the mean zonal winds along cylinders parallel to Titan's rotation axis (*16*). The derived zonal winds (Fig. 1D) were weakest at high southern latitudes and increased northward. The maximum winds were at low and mid- northern latitudes, reaching 160 m s^{-1} between 20°

[1]NASA/Goddard Space Flight Center, Code 693, Greenbelt, MD 20771, USA. [2]Science Systems and Applications, 5900 Princess Garden Parkway, Suite 300, Lanham, MD 20706, USA. [3]Department of Astronomy, Cornell University, Ithaca, NY 14853, USA. [4]Department of Astronomy, University of Maryland, College Park, MD 20742, USA. [5]Laboratoire d'Études Spatiales et d'Instrumentation en Astrophysique (LESIA), CNRS–Unité Mixte de Recherche (UMR) 8109, Observatoire de Paris, 5 place Jules Janssen, F-91925 Meudon Cedex, France. [6]Atmospheric, Oceanic, and Planetary Physics, Clarendon Laboratory, Parks Road, University of Oxford, Oxford OX1 3PU, UK. [7]QSS Group, 4500 Forbes Boulevard, Suite 200, Lanham, MD 20706, USA. [8]Department of Earth and Planetary Science, Johns Hopkins University, Baltimore, MD 21218, USA. [9]Jet Propulsion Laboratory, 4800 Oak Grove Drive, Pasadena, CA 91109, USA. [10]University of Hawaii, Institute of Astronomy, 2680 Woodlawn Drive, Honolulu, HI 96822, USA. [11]Department of Space Studies, Southwest Research Institute, 1050 Walnut Street, Suite 400, Boulder, CO 80302, USA. [12]Search for Extraterrestrial Intelligence (SETI) Institute, 515 North Whisman Road, Mountain View, CA 94043, USA. [13]Commissariat de l'Énergie Atomique, Saclay, Service d'Astrophysique, 91191 Gif-sur-Yvette Cedex, France. [14]NASA/Marshall Space Flight Center, SD50 NSSTC, Huntsville, AL 35812, USA. [15]Laboratoire Interuniversitaire des Systèmes Atmosphériques, Université de Paris 7 and 12, CNRS-UMR 7583, 61 Avenue General de Gaulle, 94010 Creteil Cedex, France. [16]Department of Physics and Astronomy, University of Cardiff, 5 The Parade, Cardiff CF24 3YB, UK. [17]Lawrence Livermore National Laboratory and Space Sciences Laboratory, University of California, Berkeley, L-041, Livermore, CA 94551, USA.

*To whom correspondence should be addressed. E-mail: f.m.flasar@nasa.gov

†Present address: LESIA, CNRS-UMR 8109, Observatoire de Paris, 5 place Jules Janssen, F-91925 Meudon Cedex, France.

and 40°N. The zonal winds at the 10-mbar level in Fig. 1D, which are not known, were set to zero. The errors from this assignment should not materially affect the displayed winds where they were strong, at low latitudes and in the north. The largest relative errors are likely to be at high southern latitudes, where the derived winds were smallest (*16*).

The CIRS observations, taken with earlier studies, indicate that the strongest zonal winds migrate seasonally in the stratosphere. Voyager infrared observations, taken in 1980 shortly after the northern spring equinox, indicated that the strongest winds were at mid- and high northern latitudes, and also at high southern latitudes (*8*). Subsequent stellar-occultation central-flash data provided information on the winds on the 0.25-mbar isobar in the upper stratosphere. An occultation of Sgr 28 in 1989, during northern summer, showed a strong jet (175 m s^{-1}) centered at 65°S (*13*, *17*). A more complex wind structure was observed in December 2001, a few months before northern winter solstice; a 220-m s^{-1} jet was centered near 60°N, and a somewhat weaker jet had a maximum near 20°S, with strong winds extending to 60°S (*18*). The CIRS data indicate that the southern-hemispheric winds have weakened and the strongest northern-hemispheric winds have migrated toward the equator (Fig. 1D). This is not a simple hemispheric reflection of the high-latitude jet observed during the Sgr 28 occultation, which occurred approximately one-half–Titan year earlier (*13*).

The lower temperatures at the south pole of Titan during early summer are in marked contrast to the south-polar warming seen in Saturn's stratosphere (*19*). A radiative explanation by itself is not straightforward, because the radiative relaxation time in Titan's upper stratosphere is so short (~1 year, compared with Saturn's orbital period of 29.5 years). Time-dependent radiative models of Titan, which assume opacities that are uniform in latitude, predict that the south pole near 1 mbar is 16 to 17 K warmer than the equator at the current season (*20*). Instead, it is 4 to 5 K colder. The gaseous opacity in the stratosphere

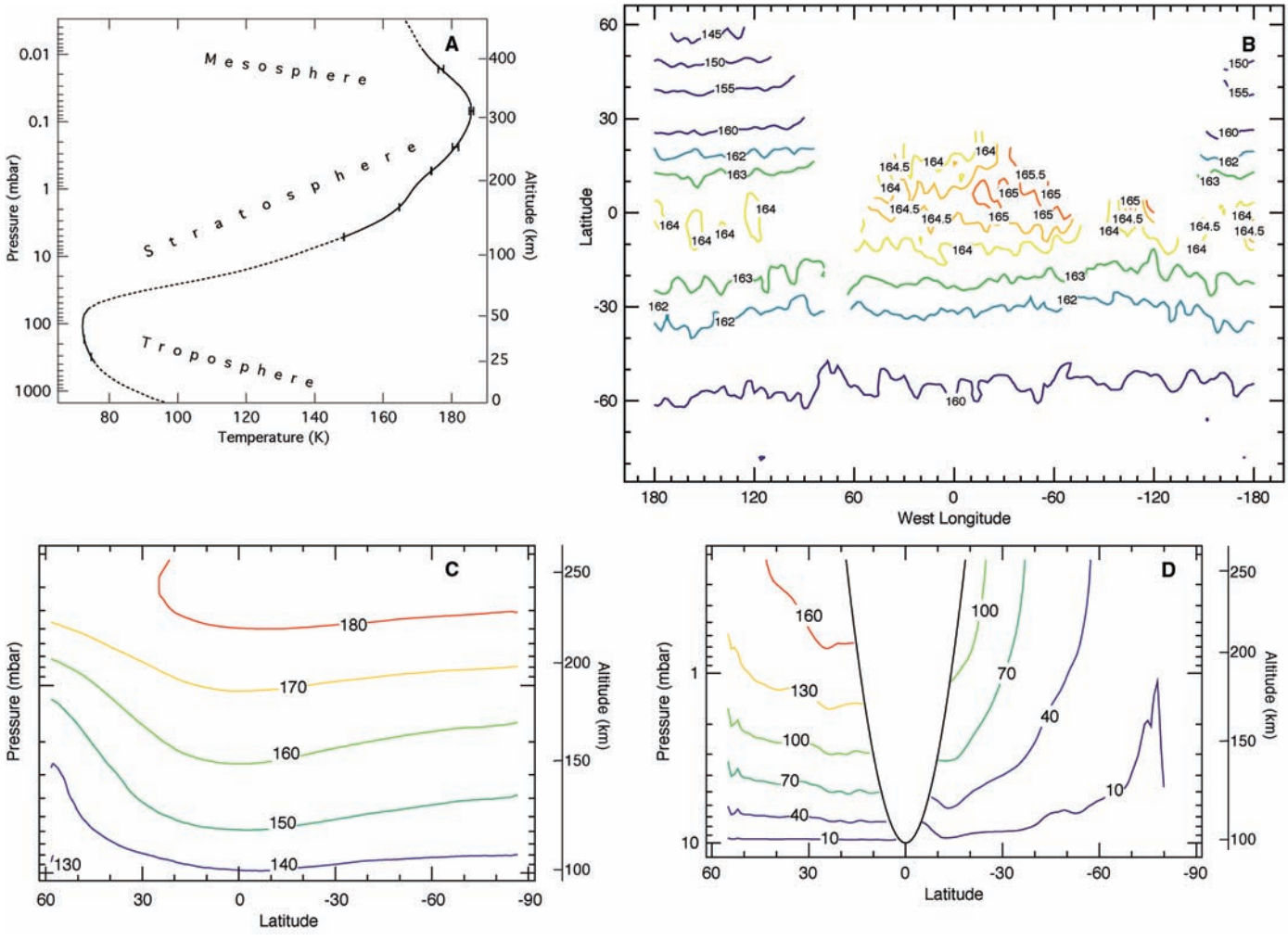

Fig. 1. Temperatures and zonal winds in Titan's atmosphere. (**A**) Vertical temperature profile near 15°S, retrieved from a combination of nadir- and limb-viewing spectra (*16*). The dashed portions of the curve represent the regions where temperatures are not well constrained by the spectra and are more influenced by the Voyager radio-occultation profiles (*1*) and radiative mesospheric models (*15*) used as the initial estimate. (**B**) Temperatures (K) on the 1.8-mbar isobar, obtained from nadir-viewing spectra at 3-cm^{-1} resolution. The map is a combination of observations taken on 2 July 2004, which were primarily in the southern hemisphere at longitudes centered near 0°, and observations on 13 December 2004, which were in both hemispheres at longitudes centered near 146°W. The horizontal resolution is 5° of great-circle arc. The temperature errors from instrument noise are 0.2 K at most locations, increasing to ~0.4 K at high northern latitudes, where there are fewer data. (**C**) Meridional cross section of stratospheric temperatures (K) averaged over available longitudes [see (B) for horizontal coverage], with latitude as the horizontal coordinate and pressure as the vertical coordinate (altitude is indicated on the right). The errors in zonal-mean temperature from noise range from 0.03 to 0.1 K. (**D**) Zonal winds (m s^{-1}), calculated from the temperatures in (C) using the thermal wind equation for a thick atmosphere (*16*). Positive numbers indicate eastward velocities. Winds at the 10-mbar level have been set equal to zero. At low latitudes within the parabola, this boundary condition is insufficient for calculating the winds, and they have been omitted (*16*). At 15° latitude, the noise in temperatures propagates into errors of 6 and 9 m s^{-1} at the 5- and 0.5-mbar levels, respectively; at higher latitudes the error decreases roughly as 1/tan (latitude).

could be heterogeneously distributed so that it cools less at low latitudes than at high latitudes, whereas fewer aerosols at the south pole could lead to less solar heating there (*21*).

The colder south pole may also be a manifestation of a lagged stratospheric cross-equatorial circulation (*8*). Although the radiative relaxation time is short compared with seasonal time scales, temperatures and zonal winds are coupled because of the thermal wind equation. The need to transport axial angular momentum from the hemisphere going into summer, where meridional temperature gradients are weakening, to that going into winter, where the gradients are strengthening, adds an inertia to the system that causes a phase lag of about one full season. It may be that the circulation is transporting angular momentum northward in early southern summer, with an attendant upwelling at high southern latitudes and adiabatic cooling. The vertical velocities required are small, about 0.05 cm s^{-1} (*16*). Two-dimensional coupled radiative-dynamical models with parameterized eddy mixing, which simulate the transport of radiatively active gaseous constituents and aerosols, have been developed to predict Titan's seasonal behavior. Although these models have been tuned to reproduce the stratospheric temperatures observed by Voyager reasonably well, they fail to account for the cooler south-polar temperatures observed now, instead predicting temperatures ~10 K warmer than at the equator (*22*).

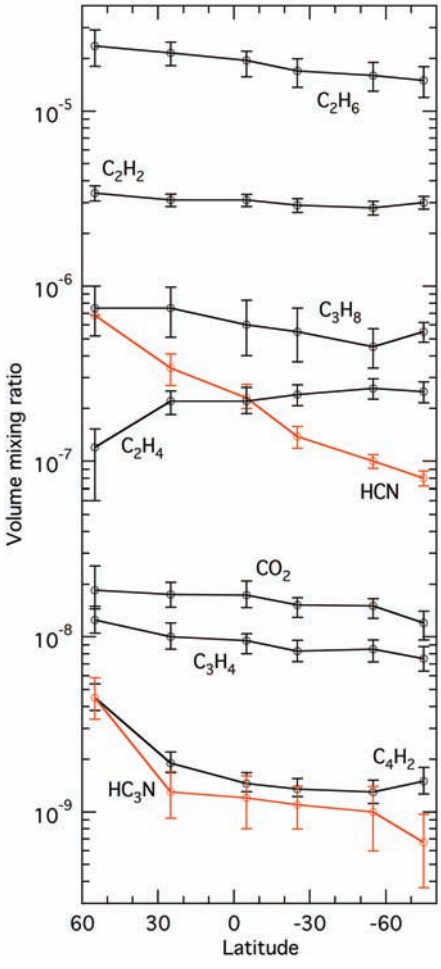

Fig. 2. Meridional distribution of several hydrocarbons and nitriles, retrieved from the spectral regions displayed in fig. S3, but at a resolution of 3 cm^{-1} (*16*). The vertical distribution of the gases was assumed to be uniform above the condensation level in the lower stratosphere. The temperature profile in Fig. 1A was used as an initial estimate, and the stratospheric temperatures were retrieved at different latitudes from radiances in the ν_4 band of CH_4. The errors indicated include those from noise in the spectral region containing the emission lines of the individual molecules, as well as from noise in the retrieved stratospheric temperatures.

Titan's atmosphere is rich in organics: hydrocarbons and nitriles (figs. S1 to S3). Hydrocarbons form from the photolytic and catalytic dissociation of CH_4. Nitriles are created by dissociation of N_2 from ultraviolet sunlight and impacts by energetic electrons from photoionization and the magnetosphere, followed by reactions with hydrocarbon radicals (*4*–*6*). Voyager 1 infrared data (*9*), which were obtained during Titan's early northern spring, showed that the concentrations of nitriles (HCN, HC_3N, and C_2N_2) and the more photochemically active hydrocarbons (C_2H_4, C_3H_4, and C_4H_2) were enhanced at high northern latitudes by factors of 10 to 100, compared with the concentrations at low latitudes. The CIRS observations in early northern winter show an enhancement of several of the same constituents at northern latitudes (Fig. 2), but by a smaller amount. Indeed, C_2H_4 now shows not an enhancement, but a twofold depletion at high northern latitudes. If the Voyager results are typical, then one can expect a build-up of the relative concentrations of these organic compounds through the winter into early spring. Numerical simulations suggest that the enhancement of these species is associated with an axisymmetric meridional circulation that subsides in the polar region during winter and early spring (*22*, *23*). Most of the enhanced species have larger mixing ratios at higher altitudes, where they are photochemically formed. Subsidence brings these enriched parcels of atmosphere down to the levels of the observed emission, ~1 to 10 mbar (*9*). Subsidence also brings the species into winter shadow, where they are shielded from further photodissociation (*24*). For the enhancements to persist at high northern latitudes, lateral mixing with the atmosphere at other latitudes must be inhibited, compared with the transport by the meridional circulation.

Titan's strong circumpolar winds (Fig. 1D) may facilitate this isolation, which is also a critical ingredient of the terrestrial Antarctic polar vortex during winter (*25*). There, the concentrations of species such as CH_4 and HF imply strong descent from the mesosphere well into the stratosphere, and these gases have sharp gradients across the polar vortex (*26*). Indeed, the whole process leading to the ozone hole within the vortex—the cold polar temperatures leading to the formation of stratospheric clouds, which denitrify the polar atmosphere by heterogeneous chemistry, liberating gaseous Cl_2; its photodissociation in the spring into Cl, which in turn irreversibly destroys O_3—requires the polar air to be isolated from the warmer, lower-latitude air that contains reactive nitrogen compounds (*25*). Planetary waves, which normally efficiently mix air masses, are unable to penetrate the polar vortex until later in spring, when polar temperatures rise and the circumpolar winds weaken. Planetary-scale waves on Titan have not been well characterized yet. The CIRS observations indicate that any thermal contrasts associated with waves are small at present. The maximum zonal variation in temperature observed in the available coverage shown in Fig. 1B is <1 to 1.5 K.

In the southern hemisphere, where it was summer, the hydrocarbons and nitriles were more uniformly distributed with latitude (Fig. 2). The numerical simulations (*23*) attribute such flat structure to rising motions in the summer hemisphere, bringing material impoverished in the trace organics from altitudes below their condensation level in the lower stratosphere. An interesting result pertains to C_2H_4. Recent analysis of Keck broad-band filter observations acquired from 1999 to 2002 suggests that C_2H_4 was 12 to 20 times as abundant in the south-polar region as at the equator (*27*). The CIRS data show little enhancement at the south pole. The relevant C_2H_4 photolysis rate [from (*28*), adapted for full illumination and $\lambda > 160$ nm] is 2×10^{-7} s^{-1}, or a 60-day lifetime for an individual molecule. Although a 12- to 20-fold enhancement in C_2H_4 could be removed in 150 to 180 days photochemically, it is not clear what caused the enhancement reported from the Keck data, because the period of observation was already middle to late spring in the southern hemisphere, a period when rising motions are predicted (*23*), and the diurnally averaged solar illumination changes slowly.

CH_4 is a condensable gas in Titan's troposphere. Analysis of Voyager's far-infrared and radio-occultation data indicate that its mole fraction near the surface ranges from 0.06 at low latitudes to 0.02 at high latitudes (*3*). The lifetime of CH_4 in Titan's atmosphere is only 4×10^7 years (*29*), and it requires a surface or interior source if the current inventory is typical of Titan's long-term history. The distribution of stratospheric CH_4 is probably uniform (*17*). Analyses of Voyager's infrared observations (in the ν_4 band of CH_4 near 1300 cm^{-1}) and radio-occultation soundings led to estimates of the CH_4 stratospheric mole fraction in the range 0.005 to 0.045 (table S1). Part of this uncertainty resulted because the CH_4 ν_4-band line-formation region is near 1 mbar, where Voyager radio-occultation data have large

errors. Uncertainties in the argon abundance and the cold-trapping constraint applied in the tropopause region also contributed to the errors in the estimated CH_4 mole fraction. The use of the pure rotational lines of CH_4 in the far-infrared (fig. S2B) eliminates many of these ambiguities. The line-formation region is in the stratosphere between 3 and 20 mbar (140 to 80 km altitude), which mostly lies between the two regions accessible to direct-temperature sounding, the upper troposphere and tropopause region between 500 and 50 mbar (20 to 60 km), and the upper stratosphere between 5 and 0.5 mbar (130 to 230 km). Nevertheless, interpolation between the two altitude ranges constrains the temperatures sufficiently to make an improved determination of the stratospheric CH_4 abundance. The optically thick ν_4 band is not too sensitive to the CH_4 abundance, but is more sensitive to the stratospheric temperatures, because it is on the Wien tail of the Planck function. The rotational lines are almost optically thin, and therefore they are more sensitive to the stratospheric CH_4 abundance but less sensitive to temperature, because they lie at wave numbers below those at the peak emission (fig. S1) (*30*). Figure S4 illustrates fits for synthetic spectra with different CH_4 mole fractions. The best fit in a least-squares sense to all the rotational lines corresponds to a mole fraction of $(1.6 \pm 0.5) \times 10^{-2}$. This is comparable to the mole fraction determined at 1000- to 1200-km altitude from remote-sensing and in situ measurements (table S1), indicating that CH_4 is fairly well mixed up to these altitudes.

In addition to containing CH_4, the far-infrared contains rotational lines of stratospheric emission from CO and HCN (fig. S2A). The rotational line-formation region of CO is similar to that of CH_4. We find from a least-squares fit of all the lines observed in independent selections of spectra from the T0 and TB flybys that the CO mole fraction is $(4.5 \pm 1.5) \times 10^{-5}$, assuming that it is uniform with altitude (*31*). This is consistent with the determination $[(5.0 \pm 1.0) \times 10^{-5}]$ by Gurwell and Muhleman (*32*), and marginally consistent with what Hidayat *et al*. (*33*) inferred below the 1-mbar level from disk-averaged heterodyne millimeter observations $[(2.5 \pm 0.5) \times 10^{-5}]$. Within the errors, it is also consistent with the tropospheric value $[(3.2 \pm 1.0) \times 10^{-5}]$ derived from 5-μm spectra (*34*), although one cannot rule out that the stratosphere has a higher concentration. One might expect the mole fractions of CO in the stratosphere and troposphere to be more or less equal, because CO does not condense at the temperatures and abundances observed, and the time constant for photochemical adjustment under current conditions is $\sim 10^9$ years (*4*).

References and Notes

1. G. F. Lindal *et al.*, *Icarus* **53**, 348 (1983).
2. D. M. Hunten *et al.*, in *Saturn*, T. Gehrels, M. S. Matthews, Eds. (Univ. of Arizona Press, Tucson, AZ, 1984), pp. 671–759.
3. R. E. Samuelson, N. R. Nath, A. Borysow, *Planet. Space Sci.* **45**, 959 (1997).
4. Y. L. Yung, M. Allen, J. P. Pinto, *Astrophys. J. (Suppl.)* **55**, 465 (1984).
5. D. Toublanc *et al.*, *Icarus* **113**, 2 (1995).
6. E. H. Wilson, S. K. Atreya, *J. Geophys. Res.* **109**, E06002, 10.1029/2003JE002181 (2004).
7. F. M. Flasar, R. E. Samuelson, B. J. Conrath, *Nature* **292**, 693 (1981).
8. F. M. Flasar, B. J. Conrath, *Icarus* **85**, 346 (1990).
9. A. Coustenis, B. Bézard, *Icarus* **115**, 126 (1995).
10. V. Kunde *et al.*, in *Cassini/Huygens: A Mission to the Saturnian Systems*, L. Horn, Ed. (SPIE Proceedings, The International Society for Optical Engineering, Bellingham, WA, 1996), pp. 162–177.
11. F. M. Flasar *et al.*, *Space Sci. Rev.* **115**, 169 (2004).
12. A. Coustenis *et al.*, *Icarus* **161**, 383 (2003).
13. W. B. Hubbard *et al.*, *Astron. Astrophys.* **269**, 541 (1993).
14. B. Sicardy *et al.*, *Icarus* **142**, 357 (1999).
15. R. V. Yelle, *Astrophys. J.* **383**, 380 (1991).
16. Materials and methods are available as supporting material on *Science* Online.
17. F. M. Flasar, *Planet. Space Sci.* **46**, 1125 (1998).
18. A. Bouchez, thesis, California Institute of Technology (2004); available at www.gps.caltech.edu/~antonin/thesis/.
19. F. M. Flasar *et al.*, *Science* **307**, 1247 (2005).
20. F. Hourdin *et al.*, *Icarus* **117**, 358 (1995).
21. B. Bézard, A. Coustenis, C. P. McKay, *Icarus* **113**, 267 (1995).
22. F. Hourdin, S. Lebonnois, D. Luz, P. Rannou, *J. Geophys. Res.* **109**, E12005, 10.1029/2004JE002282 (2004).
23. S. Lebonnois, D. Toublanc, F. Hourdin, P. Rannou, *Icarus* **152**, 384 (2001).
24. Y. L. Yung, *Icarus* **72**, 468 (1987).
25. M. R. Schoeberl, M. R. Hartman, *Science* **251**, 46 (1991).
26. J. T. Bacmeister, M. R. Schoeberl, M. E. Summers, J. R. Rosenfeld, X. Zhu, *J. Geophys. Res.* **100**, 11669 (1995).
27. H. G. Roe, I. de Pater, C. P. McKay, *Icarus* **169**, 440 (2004).
28. J. I. Moses *et al.*, *Icarus* **143**, 244 (2000).
29. D. Strobel, *Planet. Space Sci.* **30**, 839 (1982).
30. A. Coustenis *et al.*, *Icarus* **102**, 240 (1993).
31. To fit the CO rotational lines, we also had to fit the HCN lines. To do so, we used the vertical profile derived by Marten *et al*. (*35*) from disk-averaged millimeter observations, but scaled by a constant factor, $2.5^{+1.5}_{-1.1}$ (where +1.5 and –1.1 are the error values) for a selection of T0 spectra centered at 7°S and 2.8 ± 1 for a selection of TB spectra centered at 17°N.
32. M. A. Gurwell, D. O. Muhleman, *Icarus* **117**, 375 (1995).
33. T. Hidayat, A. Marten, B. Bézard, D. Gautier, *Icarus* **133**, 109 (1998).
34. E. Lellouch *et al.*, *Icarus* **162**, 125 (2003).
35. A. Marten, T. Hidayat, Y. Biraud, R. Moreno, *Icarus* **158**, 532 (2002).
36. S. Albright, M. H. Elliott, and J. S. Tingley assisted with instrument commanding and data processing; D. Crick, M. de Cates, and S. Brooks assisted with observation designs; and N. Stone helped with data analysis. We acknowledge support from the NASA Cassini Project, the British Particle Physics and Astronomy Research Council, the Centre National d'Études Spatiales (CNES), and the Institut National des Sciences de l'Univers (CNRS/INSU).

Supporting Online Material
www.sciencemag.org/cgi/content/full/308/5724/975/DC1
Materials and Methods
Figs. S1 to S4
Table S1
References

16 February 2005; accepted 14 April 2005
10.1126/science.1111150

REPORT

The Cassini UVIS Stellar Probe of the Titan Atmosphere

Donald E. Shemansky,[1]* A. Ian F. Stewart,[2] Robert A. West,[3] Larry W. Esposito,[2] Janet T. Hallett,[1] Xianming Liu[1]

The Cassini Ultraviolet Imaging Spectrometer (UVIS) observed the extinction of photons from two stars by the atmosphere of Titan during the Titan flyby. Six species were identified and measured: methane, acetylene, ethylene, ethane, diacetylene, and hydrogen cyanide. The observations cover altitudes from 450 to 1600 kilometers above the surface. A mesopause is inferred from extraction of the temperature structure of methane, located at 615 km with a temperature minimum of 114 kelvin. The asymptotic kinetic temperature at the top of the atmosphere determined from this experiment is 151 kelvin. The higher order hydrocarbons and hydrogen cyanide peak sharply in abundance and are undetectable below altitudes ranging from 750 to 600 km, leaving methane as the only identifiable carbonaceous molecule in this experiment below 600 km.

On 13 December 2004, the Cassini UVIS observed the occultation of two stars, Shaula (λ Sco) and Spica (α Vir) near the end of the second Titan flyby (labeled T_B). Both measurements of atmospheric transmission were obtained in egress: Spica was in the northern hemisphere over a range of latitudes and Shaula at a southern latitude, –36° (fig. S1). Observations were made with the extreme ultraviolet (EUV) and the far ultraviolet (FUV) UVIS channels (*1*). Data from Spica were compromised by spacecraft pointing drift but provide useful comparative atmospheric structural information at lower altitudes (*2*). The spectral range of the FUV observations (110 nm to 190 nm) is effective for the identification and determination of the hydrocarbon species abundances. These complement and extend solar occultation results from Voyager 1 and 2 in 1980 to 1981 (*3*, *4*) into the range 900 to 1200 km for CH_4. Our data